Dynamics of branched domain structures

M. Gabay and T. Garel
Laboratoire de Physique des Solides, Bâtiment 510, Université Paris—Sud, Centre d'Orsay, 91405 Orsay Cédex, France

(Received 2 December 1985; revised manuscript received 22 January 1986)

We consider Ising dipolar ferromagnets in a simple geometry (infinite slab of thickness D). When D increases, these systems undergo phase transitions characterized by the appearance of branched domain structures. We have studied the field-induced distortions of the highly branched case, in the framework of the self-similar Privorotskii model. This enables us to calculate the response of the system to a small field step, using a constrained dynamical model of Palmer *et al.* Relaxations follow a $\ln t$ law. This behavior is to be contrasted to the stripe (unbranched) case, where a usual exponential relaxation is obtained. This slowing down can be traced back to the existence of many length scales in the branched regime. Analogous results should hold for dipolar metamagnets.

I. INTRODUCTION

The study of size effects in dipolar ferromagnets and metamagnets yields additional insight into the properties of frustrated systems. For materials such as $BaFe_{12}O_{19}$ (Ref. 1) or $FeCl_2$ (Ref. 2), the source of frustration is the competition between short-range exchange interactions and long-range dipolar interactions. As a result, the ground state consists of a complicated domain structure. To simplify the analysis, we only consider samples of thickness $L_z=D$, confined between two plates of infinite planar extent ($L_x, L_y \to \infty$). Furthermore, we shall focus our attention on strongly uniaxial (Ising) magnets. The Ising axis is then chosen to lie in the z direction. Since our conclusions apply to both the ferromagnetic and metamagnetic cases, we will only consider ferromagnetic dipolar magnets.

At zero temperature ($T=0$ K), in the absence of an external magnetic field H, a commonly observed structure[1,3] is the stripe structure where up and down domains alternate with a periodicity d [Fig. 1(a)]. This periodicity results from a balance between the gain in surface magnetostatic energy, when the domain structure is formed, and the cost of creating domain walls. Indeed, one finds[1,4] $d \sim (D\delta)^{1/2}$, where the characteristic length δ is the ratio between the wall energy per unit area and the magnetostatic energy per unit volume. Neglecting wall undulations[5,6] (we shall come back to this point in the discussion), the stripe structure remains stable up to $D=D_c^{(1)} \simeq 30\delta$. For $D \gtrsim D_c^{(1)}$, a branching instability develops[7] in the stripe structure [Fig. 1(b)]. Beyond $D_c^{(1)}$, the additional cost in wall and bulk magnetostatic energies in the branched structure is more than offset by the large extra reduction in surface magnetostatic energy. As D is increased further, N branching generations develop in succession through second-order transitions, at $D_c^{(2)}, \ldots, D_c^{(N)}$ [Fig. 1(c)].

For very large D, the ground state of the branched pattern consists of layered periodic structures, the periodicity $d(z)$ of which varies quasicontinuously with z:

$$d_0 \leq d(z) \leq d \ , \tag{1}$$

where $d_0 \sim \delta$ is the surface periodicity and $d \sim (D^2\delta)^{1/3}$ is the periodicity deep inside the bulk. In this limit, the almost infinite number of branching generations has generated an almost infinite number of length scales. Furthermore, since the surface magnetostatic energy of the system is proportional to d_0, and since $d_0 \ll d$, branching

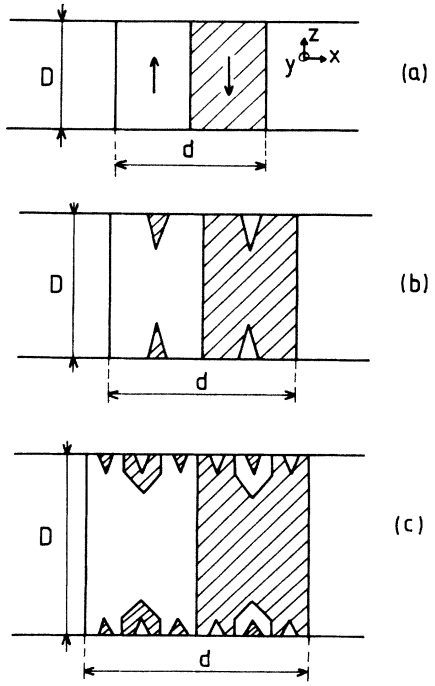

FIG. 1. (a) Stripe phase: down spins are indicated by the hatched areas. (b) Stage 1 of the branching process ($D_c^{(1)} < D < D_c^{(2)}$). The triangular shape of the spikes is only an approximation (see Ref. 7). (c) Stage 2 of the branching process ($D_c^{(2)} < D < D_c^{(3)}$).

has achieved a very effective reduction of the energy [see Eq. (4d) below]. One may say that it is the physical mechanism by which the source of frustration—the magnetic poles on the surface—is screened.

II. THE PRIVOROTSKII MODEL FOR $H=T=0$

To study the statics and dynamics of very ramified structures, we shall use a model due to Privorotskii.[8] In this model, the ground state of an N-ly branched pattern consists of a self-similar structure of $(N+1)$ layers (Fig. 2) such that the following is true.

(i) The periodicity in the kth layer is $d_k=d/3^k$ for $k=0,1,2,\ldots,N$ (d denotes the bulk periodicity).

(ii) The width of the branched regions in the kth layer is $d_{k-1}/6$ $(k\geq 1)$. For instance, in Fig. 2, one has $W_{AC}=d/6$ (layer 1) and $W_{A'C'}=d/18$ (layer 2).

(iii) The thickness of the kth layer is $l_k=l_1/\lambda^{k-1}$ for $k=1,2,\ldots,N$. This value of l_k is obtained through minimization of the l_k-dependent part of the energy in Privorotskii's model (PM), and we have[7(c)]

$$l_1=\frac{1}{3}\left[\frac{\pi}{2}\right]^{1/2}\left[1-\left[\frac{2}{3}\right]^{3/2}\right]\frac{d^{3/2}}{\delta^{1/2}}$$

and

$$\lambda=3^{3/2}\,.$$

Properties (i) and (ii) allow a very effective reduction of the surface magnetostatic energy, for all N. Property (ii), however, implies a high volume energy and, as a result, the energy of PM is higher than that obtained from a (more rigorous) variational calculation of the ground-state structure.[7(c),9] Yet, as N increases, the characteristics of the variational solution approach those of PM; also, the variational method becomes rapidly cumbersome, whereas the Privorotskii scheme allows an easy computation of the relevant quantities, for all N. This is our justification for using PM in the large-N limit, as a reasonable approximation to the true ground state. For $H=T=0$, the nonextensive part of PM energy reads as[10]

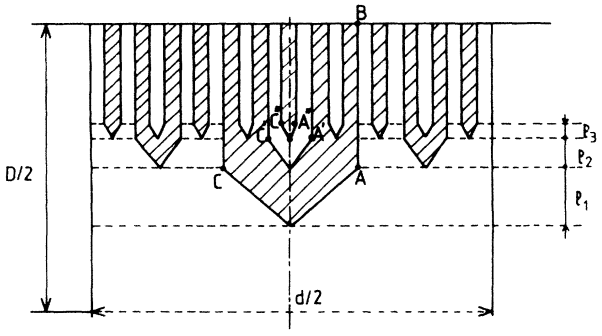

FIG. 2. Privorotskii model. Three generations of branching are shown in the upper half of a domain of up spins. The second generation (l_2) grows when $W_{AC}=\frac{1}{3}(d/2)$, the third generation (l_3) when $W_{A'C'}=W_{AC}/3$, the fourth generation (l_4) when $W_{A''C''}=W_{A'C'}/3$, etc.

$$\epsilon_N(H=0)=\frac{E_N(H=0)}{L_xL_y}=\epsilon_w+\epsilon_S+\epsilon_V\,, \tag{2}$$

where (i) the wall energy of the underlying stripe structure is

$$\epsilon_w=2\sigma_w\frac{D}{d}\,, \tag{3a}$$

σ_w is the surface tension, (ii) the surface magnetostatic energy is

$$\epsilon_S=\frac{8}{\pi^2}m_1^2dX_N^2 \tag{3b}$$

with $X_N^2=3^{-N}$; m_1 is the bulk magnetization, and (iii) the volume energy due to branching is

$$\epsilon_V=\mu m_1^2(\delta d)^{1/2}\left[\tfrac{4}{5}(1+y)-X_N+\tfrac{1}{5}(1-4y)X_N^3\right]$$

with

$$\mu=\frac{20}{3}\left[\frac{\pi}{2}\right]^{1/2}\frac{[1-(\frac{2}{3})^{3/2}]}{(1-3^{-1/2})}\,,\quad \delta=\frac{\sigma_w}{m_1^2}\,,$$

and from Ref. 11,

$$y=\frac{1}{2(3\sqrt{3}-1)}\,. \tag{3c}$$

For large D—that is for large N—minimization with respect to d and N yields

$$d\sim D^{2/3}\delta^{1/3} \tag{4a}$$

and

$$N\sim\ln\frac{D}{\delta}\,. \tag{4b}$$

This in turn gives

$$\epsilon_N(H=0)\sim m_1^2(\delta^2D)^{1/3}\,. \tag{4c}$$

Equations (4a)–(4c) confirm that in the $N\to\infty$ limit, one has

$$\epsilon_w\sim\epsilon_V\gg\epsilon_S\sim m_1^2\delta\,. \tag{4d}$$

This situation is to be compared with the stripe case where $\epsilon_w\sim\epsilon_S\sim m_1^2(\delta D)^{1/2}$.

III. DISTORTIONS OF THE BRANCHED STRUCTURE IN A FIELD

Applying a magnetic field H in the z direction creates an asymmetry between up and down domains. Denoting by d_1 (d_2) the width of an up (down) domain in the bulk, we characterize the asymmetry, in an N-ly ramified structure, by

$$\Delta\xi_N=\frac{d_1-d_2}{2d} \tag{5}$$

with $d=d_1+d_2$. For large N, the sequence of distortions generated as H is increased, in inferred from the results of the variational approach, used for small N.[9] In that small-N limit, one observes three regimes.

(a) For small H, $\Delta\xi_N$ increases linearly with H; d as well as the other parameters characterizing the branched structure retain their $H=0$ value.

(b) Beyond a threshold field H_0, the system undergoes a first-order phase transition to a state with one less generation of spikes.

(c) For large enough H, the branched structure gives way to a stripe structure.

Regimes (a) and (b) are clearly seen to result from the competition between the screening effect mentioned earlier and the Zeeman effect. The former favors $\Delta\xi_N=0$, whereas the latter favors $\Delta\xi_N \gg 0$. The compromise is a $\Delta\xi_N>0$ and a rearrangement of the positions of the domains, to achieve the lowest possible ϵ_S. Similarly, beyond H_0, the system goes from an N-ly to an $(N-1)$-ly branched structure, which still allows a fairly effective screening. This also lowers the Zeeman energy, inasmuch as $\Delta\xi_{N-1}>\Delta\xi_N$ (as we show below). Since the importance of the screening effect increases as N grows, we shall *assume* that regime (a) exists in the large-N limit, and work out some of its characteristics within PM, as well as its range of validity. These results will be used in Sec. IV, where we study dynamical effects. In regime (a), one may write the energy of PM as

$$\epsilon_N(H)=\epsilon_N(0)+\Delta\epsilon_S-HDm_1\Delta\xi_N\ , \tag{6a}$$

where

$$\Delta\epsilon_S=\frac{8}{\pi^2}m_1^2 d\left[\sum_{n=1}^{\infty}\frac{a_n^2}{n}-X_N^2\right]+2\pi Dm_1^2(\Delta\xi_N)^2\ . \tag{6b}$$

In Eq. (6b), d is the zero field value of the bulk periodicity, and a_n depends explicitly upon $\Delta\xi_N$ and upon (3^N-1) parameters describing the displacements of the centers of all the spikes with respect to their $H=0$ configuration. Since these parameters appear only in $\Delta\epsilon_S$, they have to be chosen so as to minimize $\Delta\epsilon_S$. A partly analytical (for small N) and partly numerical approach (for large N) shows that (i) blocks of spins such as those shown in Fig. 3 move cohesively, (ii) the displacements of blocks containing the same number p of generations (p-blocks) are equal in magnitude, and (iii) the displacement of the two central blocks are zero, for symmetry reasons.

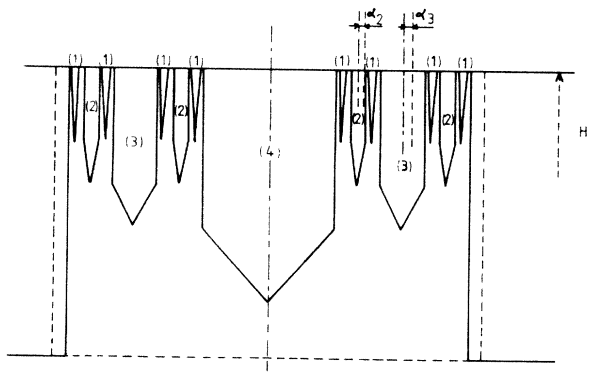

FIG. 3. Shift of the branched pattern in the presence of a magnetic field H. Half a domain is shown with $N=4$ generations. The boundary walls (dashed lines) are shifted by $\frac{1}{2}(d\Delta\xi_4)$. The central 4-block does not move for symmetry reasons, the two 3-blocks are shifted (in opposite directions) by $(\alpha_3 d\Delta\xi_4)$, the four 2-blocks by $(\alpha_2 d\Delta\xi_4)$, and the eight 1-block by $(\alpha_1 d\Delta\xi_4)$ (not shown in the figure).

These properties reduce the number of parameters to $N-1$ (not counting $\Delta\xi_N$) and we denote these parameters by $\alpha_1,\alpha_2,\ldots,\alpha_{N-1}$. [The shift of a p-block is written as $\alpha_p(d\Delta\xi_N)$.] In terms of the $\{\alpha_p\}$, the coefficient a_n of Eq. (6b) can be calculated as

$$a_n=\frac{1}{n}\left[(-1)^N\frac{\sin(n\pi)}{2\cos x_N}+2\sin\left[\frac{n\pi}{2}\Delta\xi_N\right]\times\cos\left[\frac{n\pi}{2}(1+\Delta\xi_N)\right]-\frac{\sin(n\pi/6)}{\cos x_N}\sum_{p=1}^{N-1}b_p\right], \tag{7}$$

where $x_N=n\pi/2\cdot 3^N$ and

$$b_p=2^{N-p+1}\sin\left[\frac{\pi n}{2}\alpha_p\Delta\xi_N\right]\cos\left[\frac{\pi n}{2}(1+\alpha_p\Delta\xi_N)\right]\times\sin[(3^{p-1}+1)x_N]c_p \tag{8a}$$

with

$$c_p=\prod_{i=p}^{N-2}\cos(2\cdot 3^i x_N)\quad\text{for } p=1,2,\ldots,N-2\ , \tag{8b}$$

$$c_{N-1}=1\ . \tag{8c}$$

Guidelines for deriving Eqs. (7) and (8) are presented in the Appendix. Using Eqs. (7) and (8), we have numerically minimized $\Delta\epsilon_S$ for a given $\Delta\xi_N$ (that is for a given H), for $N\leq 9$ branching generations. We find that

$$\alpha_p=\frac{\alpha_1}{2^{p-1}}\quad\text{for } p=1,2,\ldots,N-1 \tag{9a}$$

and

$$\alpha_1\simeq\frac{\alpha_0}{2^{N-1}}\quad\text{for } N\geq 2\ . \tag{9b}$$

(The value of the numerical constant α_0 depends upon the parity of N.) Using (9) we can write (6a) as

$$\epsilon_N(H)=\epsilon_N(0)+m_1^2(2\pi D-K_N d)(\Delta\xi_N)^2-m_1 HD\Delta\xi_N\ , \tag{10}$$

where K_N is a finite positive constant. We therefore have

$$\Delta\xi_N=\frac{1}{2[2\pi-K_N(d/D)]}\frac{H}{m_1}\ , \tag{11}$$

which shows that $\Delta\xi_N$ decreases when D increases (in other words, one has $\Delta\xi_N<\Delta\xi_{N-1}$). We now proceed to determine the range of fields for which regime (a) can exist. Using (10) and (11), we have

$$\epsilon_N(H)=\epsilon_N(0)-\frac{1}{4[2\pi-K_N(d/D)]}H^2D\ . \tag{12}$$

In the large-N limit, we have

$$\epsilon_N(0) \sim m_1^{\frac{2}{3}}(D\delta^2)^{1/3} \sim \epsilon_w \sim \epsilon_V \ .$$

In order for d and the other relevant parameters to retain their $H=0$ value, one must have

$$\epsilon_N(0) \gg \frac{1}{4[2\pi - K_N(d/D)]} H^2 D$$

that is

$$\frac{H}{m_1} \ll \left[\frac{\delta}{D}\right]^{1/3} . \tag{13}$$

IV. DYNAMICS: RESPONSE TO A FIELD STEP

In this section, we consider the low-temperature response of a very ramified structure to a small field step around $H=0$: $h(t)=h$ for $t>0$ and $h(t)=0$ for $t<0$. If the temperature is low enough, the preceding results should apply; to avoid unnecessary complications, we take

$$\frac{h}{m_1} \ll \left[\frac{\delta}{D}\right]^{1/3} .$$

Due to the fact that the static response to a field is dictated by a balance between the screening and Zeeman effects, we propose a simple scenario for the dynamics of the system: the distortion propagates in time, from the bulk to the surface, in discrete steps (Fig. 4). The justification for this scheme is twofold.

(1) The system decreases its energy through the Zeeman term without increasing ϵ_S at the same time, until the final step.

(2) The layer-by-layer response to a change in $d(z)$ is consistent with PM, which can be viewed as a piling up of N singly branched structures.[7,8] The progressive relaxation process preserves the different length scales (l_k) involved in the magnetostatic bulk energy, and is less costly than a global rearrangement.

To describe the type of distortions we propose, we build a hierarchically constrained model based on that of Palmer *et al.*[12] Within PM, $\mathcal{N}$ spins are distributed among $N+1$ layers. A layer indexed by k ($k=0,1,2,\ldots,N$) contains N_k spins ($\sum_k N_k = \mathcal{N}$). According to the "reptation" scheme, the relaxation from layer k to layer $k+1$ may only take place if the μ_k "active spins" in layer k have relaxed: The process at level k is completed when the spikes at level k have shifted by an amount equal to the *static* displacements [Eq. (9)]. For a half period, we have

$$N_k = \frac{1}{b^3} L_y dl_k \quad \text{for } k=1,2,\ldots,N \tag{14a}$$

and

$$N_0 = \frac{1}{b^3} L_y d \left[\frac{D}{2} - l\right] \tag{14b}$$

with $l=\sum_{k=1}^{N} l_k$; b is the lattice spacing and $\mathcal{N}=(1/2b^3)L_y dD$. From Fig. 4 and using Eqs. (9) for the various $\{\alpha_p\}$ involved in the displacement of the spikes at level k, we have

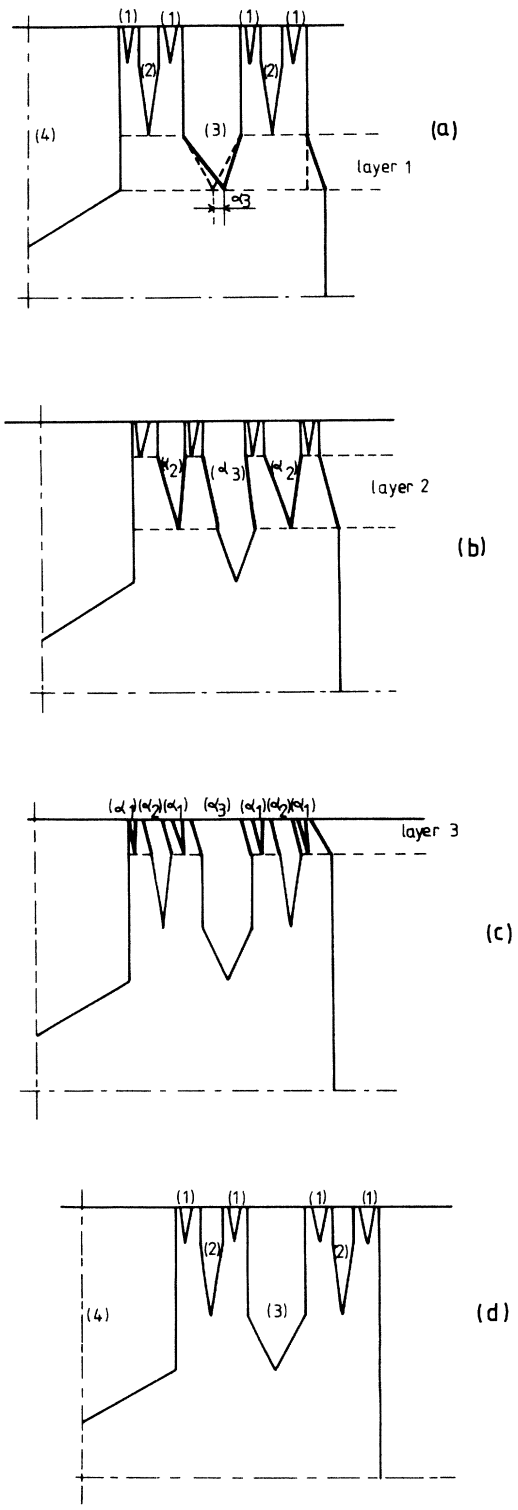

FIG. 4. Illustration of the four stages of the reptation process for $N=4$. Only part of an up domain is shown and the inner spikes of the 3- and 2-blocks are not indicated. The "active spins" at each step are shown as heavy-solid lines (a). In layer 1 (l_1) relaxation implies a shift ($\alpha_3 d\Delta\xi_4$) of the 3-block and a shift ($\frac{1}{2}d\Delta\xi_4$) of the boundary wall. (b) Motion of layer 2 (l_2). Note that in the calculation of the μ_2 "active spins", one must consider α_2 and α_3. (c) Motion for layer 3 (l_3). One must consider α_1, α_2, and α_3 to compute μ_3. (d) Final stage.

$$\mu_k=\frac{2}{b^3}L_y l_k d\Delta\xi_N + \frac{1}{b^3}L_y l_k d\Delta\xi_N \frac{\alpha_0}{2^{2N-k-2}} \times\left[3\cdot 2^{k-1}+\frac{1}{2^{k-1}}\sum_{p=1}^{k-3}2^{2p}(3^{k-p-1}+1)\right] . \quad (15)$$

For large N, we get

$$\mu_k\simeq\frac{2}{b^3}L_y l_k d\Delta\xi_N\left[1+\frac{16}{3}\frac{\alpha_0}{2^{2(N-k)}}\right] . \quad (16)$$

We therefore have

$$\frac{\mu_k}{N_k}\sim\Delta\xi_N\ll 1 .$$

The relaxation of the magnetization can then be written as[12]

$$\delta m(t)=\sum_k w_k e^{-t/\tau_k} \quad (17)$$

with

$$w_k=\frac{N_k}{\mathcal{N}}=\frac{2l_k}{D} , \quad (18a)$$

$$\tau_{k+1}=2^{\mu_k}\tau_k . \quad (18b)$$

The relaxation times τ_k range from $\tau_{\min}=\tau_0$ (the characteristic time for a spin flip in the stripe phase) to $\tau_{\max}=\tau_0 2^{\mathcal{S}}$ where $\mathcal{S}=\sum_{k=0}^{N-1}\mu_k$. For large N, $\tau_{\max}/\tau_0\sim e^{\Gamma}\gg 1$ since $\Gamma\sim d\,DL_y\Delta\xi_N/b^3$. Thus, for times t such that $\tau_{\min}\ll t\ll\tau_{\max}$,

$$\delta m(t)\sim\frac{w_1}{\Gamma\ln\lambda}\int_{t/\tau_{\max}}^{t/\tau_{\min}}e^{-u}\frac{du}{u} \sim\frac{w_1}{\Gamma\ln\lambda}\left[-\mathscr{C}-\ln\frac{t}{\tau_{\max}}\right] , \quad (19)$$

where $\mathscr{C}\simeq 0.577\,215$ is Euler's constant. Equation (19) shows that one expects a logarithmic approach to equilibrium for highly branched systems.

V. SUMMARY AND DISCUSSION

Within the self-similar Privorotskii model, we have studied the static and dynamic response of a very ramified structure, subjected to a magnetic field H. For small H, we have inferred the existence of a regime where two competing effects are of equal importance, namely the Zeeman effect and the screening effect (reduction of the surface magnetostatic energy due to branching). In that regime, the distortion consists of a mere rearrangement of the positions of the spikes: the shapes and sizes of the spikes as well as the bulk periodicity d retain their $H=0$ value (for instance, $d\sim\delta^{1/3}D^{2/3}$). The field range where this regime holds is a decreasing function of D (i.e., of the number N of branching generations). In a constrained dynamic model, where this rearrangement propagates from the bulk to the surface, we find that the overall magnetization relaxes toward equilibrium with a $\ln t$ law. This behavior clearly originates from the very large number of characteristic length scales obtained for large N; it should be contrasted with the stripe case, where the existence of a single scale entails an exponential relaxation.

Dipolar ferromagnets (as well as metamagnets) can be roughly divided in two categories: in the former, the ordering is mainly due to exchange interactions; dipolar interactions are only relevant for the formation of domains. These materials, such as $BaFe_{12}O_{19}$, are therefore expected to have a large characteristic length δ ($\delta\simeq 0.2$ μm), and are not expected to show more than one or two generations of branching for usual thicknesses ($D\lesssim 100$ μm). On the contrary, in the latter category, dipolar interactions also participate in the ordering process, and one may expect δ to decrease by 2 (or more) orders of magnitude; these materials, such as $LiTbF_4$,[13] should then be more appropriate to the study of very branched structures.

Lastly, let us stress that, to make our dynamical treatment more quantitative, one should include other significant processes such as wall undulations[5,6] which allow a reduction in ϵ_w, or pinning of the domain walls by (nonmagnetic) impurities.[14] For larger magnetic field steps, one should also consider possible changes between the initial and final numbers of branched generations.

ACKNOWLEDGMENTS

We thank J. Ferré for discussions and financial support. The Laboratoire de Physique des Solides is "laboratoire associé au Centre National de la Recherche Scientifique."

APPENDIX

Let us consider, for the sake of simplicity the case $N=3$ (Fig. 2). In zero applied field ($\Delta\xi_3=0$), one can easily calculate the coefficient a_n of Eq. (6b). Considering the distribution of magnetic poles on the surface, we have

$$a_n(\Delta\xi_3=0)=\frac{1}{n}\left[-\sin\frac{n\pi}{2\cdot 3^3}+\sin 3\frac{\pi n}{2\cdot 3^3} -\sin 5\frac{n\pi}{2\cdot 3^3}+\cdots-\sin 53\frac{n\pi}{2\cdot 3^3}\right] . \quad (A1)$$

That is

$$a_n(\Delta\xi_3=0)=\frac{1}{n}\sum_{k=1}^{3^3}(-1)^k\sin(2k-1)x_3$$

or

$$a_n(\Delta\xi_3=0)=-\frac{1}{n}\frac{\sin(n\pi)}{2\cos x_3} \quad (A2)$$

with $x_3=n\pi/2\cdot 3^3$. In a nonzero applied field ($\Delta\xi_3\neq 0$), one has to take into account the shifts ($\alpha_1 d\Delta\xi_3$) and ($\alpha_2\Delta\xi_3$) of the 1- and 2-blocks. Note that the central 3-

block does not move for symmetry reasons. The various terms in Eq. (A1) break into several groups: (i) those belonging to a 1-block [for instance we have $\sin(11n\pi/2\cdot 3^3+n\pi\alpha_1\Delta\xi_3)$], (ii) those belonging to a 2-block [for instance we have $\sin(15n\pi/2\cdot 3^3+n\pi\alpha_2\Delta\xi_3)$], (iii) those belong to the 3-block [for instance we have $\sin(7n\pi/2\cdot 3^3)$], and (iv) the boundary wall term is $\sin(27n\pi/2\cdot 3^3+n\pi\Delta\xi_3)$. Writing $a_n(\Delta\xi_3)=a_n(0)+[a_n(\Delta\xi_3)-a_n(0)]$ and collecting the various α_1 and α_2 contributions yields

$$
\begin{aligned}
a_n(\Delta\xi_3)=a_n(0)+[&\sin(11x_3+n\pi\alpha_1\Delta\xi_3)-\sin(11x_3)-\sin(13x_3+n\pi\alpha_1\Delta\xi_3)\\
&+\sin(13x_3)+\sin(23x_3+n\pi\alpha_1\Delta\xi_3)-\sin(23x_3)-\sin(25x_3+n\pi\alpha_1\Delta\xi_3)\\
&+\sin(25x_3)-\sin(29x_3+n\pi\alpha_1\Delta\xi_3)+\sin(29x_3)+\sin(31x_3+n\pi\alpha_1\Delta\xi_3)\\
&-\sin(31x_3)-\sin(41x_3+n\pi\alpha_1\Delta\xi_3)+\sin(41x_3)+\sin(43x_3+n\pi\alpha_1\Delta\xi_3)\\
&-\sin(43x_3)]+[\sin n\pi(\tfrac{1}{2}+\Delta\xi_3)-\sin(n\pi/2)]\\
+[&\sin(15x_3+n\pi\alpha_2\Delta\xi_3)-\sin(15x_3)-\sin(17x_3+n\pi\alpha_2\Delta\xi_3)\\
&+\sin(19x_3+n\pi\alpha_2\Delta\xi_3)-\sin(19x_3)-\sin(21x_3+n\pi\alpha_2\Delta\xi_3)+\sin(21x_3)\\
&-\sin(33x_3+n\pi\alpha_2\Delta\xi_3)+\sin(33x_3)+\sin(35x_3+n\pi\alpha_2\Delta\xi_3)-\sin(35x_3)\\
&-\sin(37x_3+n\pi\alpha_2\Delta\xi_3)+\sin(37x_3)+(39x_3+n\pi\alpha_2\Delta\xi_3)-\sin(39x_3)]\ .
\end{aligned}
\tag{A3}
$$

Rearranging (A3) and using (A2), we obtain Eqs. (7) and (8) for the case $N=3$. The extension to general N is straightforward.

[1] J. Kooy and U. Enz, Philips Res. Rep. **15**, 7 (1960).

[2] J. Hirte, H. Weitzel, and N. Lehner, Phys. Rev. B **30**, 6707 (1984); W. P. Wolf in *Proceedings of the NATO Advanced Study Institute, Geilo, 1983* (Plenum, New York, 1984); R. Bruinsma and G. Aeppli, Phys. Rev. B **29**, 2644 (1984).

[3] J. F. Dillon, E. Y. Chen, H. J. Guggenheim, and R. Alben, Phys. Rev. B **15**, 1422 (1977).

[4] C. Kittel, Rev. Mod. Phys. **21**, 541 (1949).

[5] M. Rosenberg, C. Tanasoiu, and V. Florescu, J. Appl. Phys. **37**, 3826 (1966).

[6] J. B. Goodenough, Phys. Rev. **102**, 356 (1956).

[7] (a) E. M. Lifshitz, J. Phys. (Moscow) **8**, 337 (1944); (b) A. Hubert, Phys. Status Solidi **24**, 669 (1967); (c) M. Gabay and T. Garel, J. Phys. Lett. **45**, L989 (1984); (d) M. Gabay and T. Garel, J. Phys. **46**, 5 (1985).

[8] I. Privorotskii, *Thermodynamic Theory of Domain Structures* (Wiley, New York, 1976).

[9] M. Gabay and T. Garel, J. Phys. C **19**, 655 (1986), and unpublished results.

[10] As is common in domain instabilities, the characteristics of the branching transitions are determined from the nonextensive part of the energy.

[11] Equation (3c) corrects Eq. (9) of Ref. 7(c), where y was omitted.

[12] R. G. Palmer, D. L. Stein, E. Abrahams, and P. W. Anderson, Phys. Rev. Lett. **53**, 958 (1984); **54**, 1965 (1985).

[13] J. Kötzler, D. Sellmann, and W. Aszmus, J. Magn. Magn. Mater. **45**, 245 (1984).

[14] D. A. Huse and C. L. Henley, Phys. Rev. Lett. **54**, 2708 (1985).